

Can Enhanced Diffusion Improve Helioseismic Agreement for Solar Models with Revised Abundances?

Joyce A. Guzik

Thermonuclear Applications Group, X-2, MS T-085, Los Alamos National Laboratory, Los Alamos, NM 87545

L. Scott Watson¹

University of Oxford, Astrophysics, 1 Keble Road, Oxford OX1 3RH, UK

and

Arthur N. Cox

Theoretical Astrophysics Group, T-6, MS B-227, Los Alamos National Laboratory, Los Alamos, NM 87545

joy@lanl.gov, lwatson@astro.ox.ac.uk, anc@lanl.gov

ABSTRACT

Recent solar photospheric abundance analyses (Asplund et al. 2004, 2005; Lodders 2003) revise downward the C, N, O, Ne, and Ar abundances by 0.15 to 0.2 dex compared to previous determinations of Grevesse & Sauval (1998). The abundances of Fe and other elements are reduced by smaller amounts, 0.05 to 0.1 dex. With these revisions, the photospheric Z/X decreases to 0.0165 (0.0177 Lodders), and Z to ~ 0.0122 (0.0133 Lodders). A number of papers (e.g., Basu & Antia 2004a,b; Montalbán et al. 2004; Bahcall & Pinsonneault 2004; Turck-Chièze et al. 2004a; Antia & Basu 2005) report that solar models evolved with standard opacities and diffusion treatment using these new abundances give poor agreement with helioseismic inferences for sound-speed and density profile, convection-zone helium abundance, and convection-zone depth. These authors also considered a limited set of models with increased opacities, enhanced diffusion, or abundance variations to improve agreement, finding no entirely satisfactory solution. Here we explore evolved solar models with varying

¹Department of Physics and Astronomy, University of New Mexico, 800 Yale Boulevard NE, Albuquerque, NM 87131

diffusion treatments, including enhanced diffusion with separate multipliers for helium and other elements, to reduce the photospheric abundances, while keeping the interior abundances about the same as earlier standard models. While enhanced diffusion improves agreement with some helioseismic constraints compared to a solar model evolved with the new abundances using nominal input physics, the required increases in thermal diffusion rates are unphysically large, and none of the variations tried completely restores the good agreement attained using the earlier abundances. A combination of modest opacity increases, diffusion enhancements, and abundance increases near the level of the uncertainties, while somewhat contrived, remains the most physically plausible means to restore agreement with helioseismology. The case for enhanced diffusion would be improved if the inferred convection-zone helium abundance could be reduced; we recommend reconsidering this derivation in light of new equations of state with modified abundances and other improvements. We also recommend considering, as a last resort, diluting the convection zone, which contains only 2.5% of the Sun’s mass, by *accretion* of material depleted in these more volatile elements C, N, O, Ne, & Ar after the Sun arrived on the main sequence.

Subject headings: Sun: abundances–Sun:interior–Sun: oscillations

1. Introduction

Recent solar photospheric abundance analyses (Asplund et al. 2004, 2005; Lodders 2003) revise downward the abundances of C, N, O, Ne, and Ar by 0.15 to 0.2 dex, compared to earlier determinations of Grevesse & Sauval (1998, hereafter GS98). Smaller decreases of 0.05 to 0.1 dex in Na, Mg, Al, P, S, K, Ca, and Fe are also derived. Asplund et al. (2005) reduce the solar photospheric Z/X to $0.0165 \pm 10\%$ (*c.f.* Lodders 0.0177) and Z to ~ 0.0122 (*c.f.* Lodders 0.0133). Standard solar models including diffusive settling that give good agreement with helioseismology have been calibrated to earlier higher abundance determinations, e.g., the GS98 values of $Z/X = 0.023$ and $Z \sim 0.0171$. In fact, even earlier published mixtures, e.g. Grevesse & Noels (1993, hereafter GN93) or Anders & Grevesse (1989), with higher Z/X of 0.0245 and 0.0275, respectively, and consequently higher opacities, would be preferable for improving agreement between calculated and inferred sound-speed profiles below the convection zone (see, e.g., Boothroyd & Sackmann 2003; Neuforge-Verheecke et al. 2001b).

A number of research groups (Basu & Antia 2004a,b; Bahcall & Pinsonneault 2004; Serenelli et al. 2004; Bahcall, Serenelli & Pinsonneault 2004; Montalbán et al. 2004; Turck-Chièze et al. 2004a; Antia & Basu 2005) conclude that solar models evolved with the

new lower abundances give worse agreement with the helioseismically-inferred sound speed and density profiles, convection-zone depth, and convection-zone helium abundance. These groups explored a limited set of models attempting to restore agreement, including models with opacity increases below the convection zone, multipliers on diffusion velocities, and increases in Z/X or individual element abundances to the upper limits of their quoted uncertainties. Asplund et al. (2004) suggest that enhanced diffusion may be able to restore the agreement with convection-zone depth, as the new abundances produce convection zones that are too shallow. Basu & Antia (2004a,b) and Montalbán et al. (2004) evolved models with multipliers on the diffusion velocities, finding that it is difficult to avoid either a convection zone that is too shallow, or a convection-zone helium abundance that is too low.

Here we present results for solar models evolved with different initial abundances and diffusion treatments than previously published to see whether we can reconcile the new abundances with helioseismology. As a variation on previous enhanced-diffusion investigations, our strategy is to attempt to retain the good sound speed profile agreement below the convection zone attained for solar models that used the earlier GN93 abundances by starting with these abundances, and then enhancing diffusion selectively of C, N, O, and Ne from the convection zone so that the present photospheric element mixture matches the new Asplund et al. (2005) mixture.

Instead of applying straight multipliers to the diffusion velocity, we consider that gravitational settling and thermal diffusion contribute about equal amounts to the diffusion velocity at the base of the convection zone (Cox, Guzik, & Kidman 1989, hereafter CGK89). Whereas gravitational settling rates may not be subject to much uncertainty, as they depend on the well-known gravitational field, the thermal diffusion treatment is more uncertain (see Paquette et al. 1986). In addition, the rates of thermal diffusion of helium, C, N, O, and other elements relative to hydrogen are not the same, and depend, for example on ionization state. Most solar models are evolved with diffusion treatments that assume complete ionization, do not include radiative levitation, and assume a dilute plasma, whereas the plasma at the base of the convection zone is in the intermediate-coupling regime, with a plasma $\Gamma \sim 1$ (CGK89). Turcotte et al. (1998) find that radiative levitation forces can be up to 40% of the gravitational force below the convection zone. They also found that the percentage of elements heavier than H and He (Z) diffused from the convection zone increases from 7.5% to as high as 10% when a detailed ionization treatment is incorporated into the diffusion calculations for individual elements. So there are several reasons to suspect that the diffusion treatment has significant uncertainties.

The diffusion treatment we apply as implemented by CGK89 follows the relative thermal, chemical, and gravitational diffusion of H, He, C, N, O, Ne, Mg and the electron sepa-

rately; therefore binary thermal resistance coefficients between elements can be adjusted to enhance the relative diffusion of individual elements with respect to hydrogen. For example, we can explore varying these rates such that we diffuse He at near the nominal rate, and enhance the diffusion of other elements that have been reduced in abundance by the new Asplund et al. (2005) mixture. While the increases in thermal diffusion coefficients that we explore are *ad hoc* and very large, at least we can determine whether modified rates are worth further investigation for reducing the discrepancy with helioseismology. We also compare our results for enhanced-diffusion models with those of Basu & Antia (2004a) and Montalbán et al. (2004).

In the recent papers listed above that attempt to reconcile the new abundances with helioseismology, either the group performs their own seismic inversion using a set of observed *p*-mode oscillation data, and reports deviations in the sound-speed or density profiles of their reference model from that inferred for the Sun, or they compare their model structure results directly to the sound-speed and density profile inversion given by, e.g., Basu et al. (2000). While Basu et al. (2000) demonstrate that the sensitivity of the inferences to the choice of reference model is small, it is also worthwhile to consider the forward method of directly comparing predicted and observed oscillation frequencies to avoid any dependence on inversion techniques. Therefore, in addition to comparing the sound speed profile and convection-zone helium abundance for our models with the seismic inferences of Basu et al. (2000) and Basu & Antia (2004a), we show direct comparisons of the observed minus calculated nonadiabatic *p*-mode frequencies for a subset of *p*-modes that propagate below the convection zone. Some of our models and results were presented at the SOHO14/GONG 2004 conference in July 2004 (Guzik & Watson 2004).

2. Solar Model Properties

For our solar model and oscillation frequency calculations, we use the codes and procedures described in Neuforge-Verhecke et al. (2001a,b) and references therein. We use the Burgers (1969) diffusive element settling treatment as implemented by CGK89 that includes thermal, gravitational, and chemical diffusion of H, He, C, N, O, Ne, and Mg. Other elements, such as Fe, are not followed explicitly, and the abundances of these are scaled with $Z=(1-X-Y)$ as the diffusion occurs. Since the elements listed above are treated individually via separate coupled equations, we can experiment with adjusting the binary thermal resistance coefficients for individual elements to allow enhanced diffusion of C, N, O, Ne, and Mg while avoiding the diffusion of too much helium (or of other elements).

We use the Lawrence Livermore National Laboratory OPAL (Iglesias & Rogers 1996)

opacities and the Alexander & Ferguson (1995) low-temperature opacities, both with the GN93 mixture. The models that we present have a photospheric Z/X somewhat larger than derived by Asplund et al. (2005). Since the GN93 mixture has less Fe relative to C, N, O, Ne, and Ar, than the Asplund et al. mixture, we are compensating for the higher relative Fe abundance of the Asplund et al. mixture by calibrating to a slightly higher Z/X . This compensation is only approximate, since different elements contribute to a greater or lesser degree to the opacity at different temperatures, with iron a large contributor near the solar center, and oxygen or neon large contributors just below the convection zone. As stated above, we have in mind the possibility of mitigating the effects of the new abundances by enhancing diffusion to bring up the oxygen (as well as the C, N, Ne, and Mg) abundance relative to Fe below the convection zone; in that case, the GN93 mixture opacities, with higher relative C, N, O, Ne, and Mg abundances, would be more representative for the mixture below the convection zone than would opacity tables constructed with the new Asplund et al. mixture. Since all of the elements are in reality diffusing at slightly different rates, the mixture is actually evolving as a function of radius and time, and so using a single mixture for the opacity tables is not strictly correct in any case, but should suffice for these exploratory calculations. We note that other modelers (e.g. Bahcall et al. 2004; Basu & Antia 2004a,b; Montalbán et al. 2004; Turck-Chièze et al. 2004a) have constructed new OPAL opacity tables for the Asplund et al. mixture (or variations they consider) for their studies, and also, to our knowledge, use tables for only one element mixture in a given model, which is valid if one assumes that all elements diffuse at the same rate.

We use the SIREFF in-line analytical equation of state (Guzik & Swenson 1997) to account for the changes in element mixtures in the EOS. However, we find that accounting for the relatively small mixture changes between GN93 and Asplund et al. in the EOS has a negligible effect on the model structure compared to the overall decrease in Z we are investigating. We use the NACRE (Angulo et al. 1999) nuclear reaction rates and standard mixing-length convection treatment (Bohm-Vitense 1958).

The models are calibrated to the present solar radius (6.9599×10^{10} cm), luminosity (3.846×10^{33} erg/s), mass (1.9891×10^{33} g), and age (4.52 ± 0.04 Gyr; Guenther et al. 1992). For future reference, we also quote here the constraints from helioseismic inversions of Basu & Antia (2004a) on the convection zone helium mass fraction Y (0.248 ± 0.003), and convection zone base radius ($0.7133 \pm 0.0005 R_{\odot}$).

We note that the initial helium abundance in solar evolution modeling is not a fixed input quantity, but is a parameter adjusted to match the solar luminosity at the present solar age. The combination of this initial abundance and the diffusion that occurs over the solar lifetime results in a convection-zone Y abundance which is then compared with the

helioseismic inference. However, this inference also depends on the equation of state for the helium ionization region in the convection zone (see, e.g., Basu & Antia 1995; Boothroyd & Sackmann 2003), although the difference in inferred Y abundance using different modern equations of state is small compared to the amount of He calculated to be depleted from the convection zone by diffusion; Basu & Antia (2004a) take into account these uncertainties due to the EOS and oscillation frequency data set in their inferred Y uncertainty estimate of ± 0.003 .

Likewise, the mixing-length to pressure-scale-height ratio is also a parameter adjusted so that the model reaches the observed solar radius at the present solar age. The convection zone depth is a property of a model calibrated in this manner, and cannot be adjusted without other adjustments in the initial abundances or input physics. There is a complex relationship between 1) the He and Z abundance that affect the opacities and equation of state, 2) diffusion below the convection zone, and 3) the mixing-length ratio required to adjust the solar model to the present radius for a fixed mass, so it is difficult to predict *a priori* the final convection-zone depth of an evolved model.

The solar convection-zone depth, and sound-speed and density profiles derived from helioseismic inversions have a small dependence on the reference models, inversion techniques, and oscillation frequency data set adopted (see, e.g., Basu, Pinsonneault, & Bahcall 2000; Basu & Antia 2004a). Again, the uncertainties in the inferences are small compared to the large differences in these quantities among calibrated evolved solar models using the new and old abundances.

3. Solar Model Comparisons

We compare six evolved models: 1) A standard solar model with GN93 abundances and standard diffusion treatment (Standard Model 1); 2) a model with reduced Z abundance close to the Asplund et al. (2005) abundances and no diffusion (Low-Z No Diffusion Model 2); 3) a model with the same initial Z as Standard Model 1, but with the binary thermal resistance coefficients for all elements (He, C, N, O, Ne, Mg) relative to H reduced by a factor of three (Enhanced Diffusion Model 3); 4) a model with the same initial Z as Standard Model 1, but with the binary thermal resistance coefficients for C, N, O, Ne, and Mg only (excepting He) relative to H reduced by a factor of seven, to enhance selectively their diffusion and avoid too much helium diffusion (Enhanced Z-Diffusion Model 4); 5) a model intermediate to Models 3 and 4, in which we lowered the binary thermal resistance coefficients for C, N, O, Ne, and Mg by a factor of four, but lowered the coefficient for He by a smaller factor of 2/3 (Intermediate Enhanced Diffusion Model 5); 6) a model with high initial Z (0.024) that consequently has

high initial Y (0.287), and binary thermal resistance coefficients for C, N, O, Ne, and Mg reduced by a factor of 15 (High-Z Enhanced Diffusion Model 6). These multipliers on the binary resistance coefficients seem very high and unphysical, but in fact are the magnitude of change in the thermal diffusion treatment required for diffusion to reduce the convection zone C, N, and O abundances from the GN93 values to near the Asplund et al. values.

Table 1 compares the initial abundances, final surface abundances, convection zone depth, and neutrino fluxes for the six models. Figure 1 compares the differences in sound-speed profile for each model with the seismic inversion of Basu et al. (2000). Figure 2 compares the observed minus calculated nonadiabatic frequency differences for each model for solar p -modes of degree $\ell=0, 2, 10,$ and 20 . The frequencies are calculated using the Pesnell (1990) code. The observed frequencies are from the BiSON group (Chaplin et al. 1996, 1998) or the LowL group (Schou & Tomczyk 1996), with the following exceptions: the two lowest frequency modes, $n=6, \ell=0$ and $n=4, \ell=2$ modes are from the SOHO/GOLF data analysis of Garcia et al. (2001), and the $\ell=0, n=8$ and $\ell=2, n=4-6$ modes are from the SOHO/MDI data analysis of Toutain et al. (1998).

4. Model Evaluation and Discussion

One can see from Table 1 and Figs. 1 and 2 that the agreement with helioseismology for the Standard Model 1 with the GN93 abundances and standard diffusion treatment and opacities is excellent, although small improvements are still needed. Suggested improvements in input physics that would remedy the small remaining sound speed differences in the solar interior include modest increases in opacity, and also introducing some mild turbulent mixing below the convection zone in or below the tachocline region that would also produce the observed Li depletion (see, e.g., Gabriel 1997; Morel, Provost, & Berthomieu 1997; Brun et al. 1999; Richard et al. 1996; Theado, Vauclair, & Richard 2001; Bahcall, Pinsonneault, & Basu 2001). Note too that our standard Model 1 convection-zone Y abundance is a little low (0.2419) compared to the Basu & Antia (2004a) seismically-determined value. The low Y value could be easily remedied by slightly decreasing the diffusion rates of our nominal CGK89 treatment, or by introducing turbulence that mixes a small amount of He back into the convection zone.

The Low-Z No-Diffusion Model 2 has the advantage that the lower Z also requires a lower initial Y (0.2493) to match the present solar luminosity. The initial (\equiv present convection zone) Y then agrees with the seismically-determined value without including any diffusion! However, this model gives poor results for the sound-speed profile below the convection zone, with discrepancies as large as 1.8%, compared to less than 0.4% for the standard model. The

convection zone of this model is also very shallow (base radius $0.7388 R_{\odot}$). These poor results are not a surprise, as even for the older, higher- Z abundances, diffusion was found to greatly improve results for standard solar models, since the decreased He abundance just below the convection zone increases the opacity below the convection zone, and the convection-zone depth. For the old abundances, diffusion was also required to decrease the convection zone Y abundance from the initial abundance needed to match the present solar luminosity.

For Model 3 with *ad hoc* lowering of the binary resistance coefficients for all elements relative to hydrogen by a factor of three, the final convection-zone Y is much too low (0.1926) compared to the inferred value, while the convection-zone Z/X is not quite low enough (0.0196) to match the Asplund et al. value, even including the 10% uncertainty. This model has a convection zone that is too deep ($0.7022 R_{\odot}$), and the sound speed discrepancies are about 0.5% below the convection zone and about 0.7% nearer the solar center. The low helium abundance, and consequent increased opacity, just below the convection zone is responsible for the very deep convection zone.

For Model 4, we attempted to avoid the problem of too much He diffusion by enhancing diffusion of selected elements only. However, for this model, the convection zone is still somewhat too shallow (base radius $0.7283 R_{\odot}$), and the surface Y is slightly low (0.2339). The sound-speed profile comparison with seismic inversions is still poor, with discrepancies just below the convection zone of about 1.3%.

Since we observe that Model 3 and Model 4 bracket the seismic results for convection-zone depth and sound-speed profile below the convection zone, for Model 5 we tried adjusting the resistance coefficients to values between those of Models 3 and 4. The sound-speed profile now agrees with the inversions almost as well as the Standard Model 1, and the convection zone is only slightly too shallow ($0.7175 R_{\odot}$). However, in this model the final Z/X ends up too high (0.0206), and the convection zone Y is somewhat low (0.2269).

Finally, considering that opacity increases improve sound-speed agreement below the convection zone (Bahcall et al. 2004; Serenelli et al. 2004; Montalban et al. 2004), we attempted to increase the opacity by increasing the initial Z of the model to 0.024, which also has the advantage of requiring a higher initial Y to match the solar luminosity. For this model, we greatly reduced the resistance coefficients for C, N, O, Ne, and Mg by a factor of 15, to deplete the convection zone Z to the observed values after 4.54 Gyr. This model has final convection zone $Z=0.0127$, and $Z/X = 0.0173$, in good agreement with the new abundances, and the final convection zone Y also remains high enough ($Y=0.2541$), as desired. However, the convection-zone depth is very shallow (base radius $0.7406 R_{\odot}$) because of the decrease in opacity below the convection zone with the increased Y, which overwhelms any opacity increases from higher Z . The resulting sound-speed profile is also in very poor

agreement with helioseismology, and is rather similar to the no-diffusion Model 2.

Figure 3 verifies that increased opacity below the convection zone correlates with decreasing convection-zone helium abundance (and deeper onset of convection) for our six calibrated models. Note that for two models, the standard Model 1 and the enhanced-diffusion Model 3 with the deepest convection zones, the higher (Model 1) or lower (Model 3) Y and Z abundances nearly compensate each other to give very similar opacity profiles below the convection zone.

Of these enhanced-diffusion models, our Model 5 shows the closest agreement with inferred sound-speed profile, convection-zone depth and p -mode frequencies. Some of the remaining discrepancies between Model 5 and the seismic inferences could be remedied by adjustments in the solar model that would also improve the higher-abundance Standard Model 1, e.g., small opacity increases, and/or including mixing below the convection zone. However, there is no justification for the large *ad hoc* lowering of the binary resistance coefficients for selected elements as applied in Model 5.

For the lowest-frequency $\ell=0$ and 2 modes compared in Fig. 2 that are least sensitive to nonadiabatic effects and inaccuracies in model surface structure, the frequency predictions agree nearly perfectly with observations for Standard Model 1 with the GN93 abundances, and for Model 5 with the tuned thermal resistance coefficients.

In addition to the p -modes that we have calculated for this paper to compare with observations, we have also calculated g -mode frequencies and growth rates (Table 3), neglecting time-dependent convection. The g -mode results have been omitted from our final journal submission, as the g -modes are most sensitive to core structure, and are not as sensitive to the solar structure just below the convection zone, where the new abundances have had the largest effect. The frequencies of these modes do not vary smoothly from mode to mode, because of the way their few nodes interact with the convection zone, where their eigenfunctions all have significant weight. The $\ell=2$ g_3 nonradial mode had a statistically-significant detection in the GOLF data analysis reported by Turck-Chièze et al. (2004b,c), with a possible detection of all three expected components at 220.12, 220.72, and 221.26 μHz . Cox & Guzik (2004) discuss upper limits on the growth rates for some g -modes, and find small positive growth rate for this mode, making it plausible that it could be observed. The predicted $\ell=2$ g_3 frequency of 221.5 μHz for the standard Model 1, as well as the predictions of enhanced-diffusion models 4, 5, and 6, are reasonably close to this observed frequency triplet. (Note that our standard Model 1 using GN93 abundances with predicted $\ell=2$ g_3 mode at 221.5 μHz is slightly different than the Model 1 discussed in Cox & Guzik (2004) with predicted frequency 221.8 μHz .) Table 3 also gives the possible $\ell=1$, g_1 frequency for all of our models; the predicted frequency for Models 1 and 5 is close to an observed strong line

at $262.2 \mu\text{Hz}$, even though the expected doublet structure for an $\ell=1$ mode is not present in the reduced data. It is less likely that any of the models' radial fundamental modes (with a predicted singlet structure) match that observed frequency.

The growth rates given in Table 3 (in parentheses) are calculated assuming frozen-in convection. Studies made with our preliminary version of time-dependent convection show that these positive growth rates produced by the hydrogen kappa effect are certainly too large, as discussed in Cox & Guzik (2004). Our best estimate for all of the Table 3 growth rates is nearly zero, since time-dependent convection and turbulent pressure effects give both positive and negative driving contributions. The single line in the SOHO spectrum at the position near the predicted $\ell=1$ g_1 mode may be the relic of a long-ago excitation, since the decay rate of the amplitude may be as long as a million years. It may be that the missing other sectoral component has decayed below detection to explain its absence today. Observationally, the radial modes are stable, but at least the fifth radial overtone seems to be seen as occasionally stochastically excited to a detectable amplitude. Other lower-order radial modes at their predicted frequencies may be observable also, but no data in the appropriate frequency ranges are published yet.

Table 2 compares the enhanced-diffusion models of Basu & Antia (2004a) and Montalban et al. (2004) with our enhanced-diffusion models. The trends are generally the same, with too-shallow convection zone depth and too-low convection zone He abundance being the problems to be overcome; the nominal Basu & Antia or Montalban et al. diffusion rates for helium appear to be somewhat lower than those for our CGK89 treatment, so their surface Y abundances are not reduced as much, but are still lower than the seismic inference. The new abundances require some means of increasing the convection-zone depth for standard physical input. The new abundances also require a slightly lower initial Y to match the solar luminosity. Reducing the He abundance in/below the convection zone by enhancing diffusion deepens the convection zone as needed, as the reduced He abundance below the convection zone dominates in raising the opacity to initiate the onset of convection. However, the helium abundance with nominal diffusion rates for our standard model already is slightly lower than the seismic value of 0.248, and therefore lowering Y and Z abundances and enhancing diffusion can only worsen this agreement. Considering these models, it does not appear likely that diffusion rates alone can be adjusted to reconcile the convection-zone depth and convection-zone helium abundance simultaneously with helioseismic constraints.

On the other hand, it is interesting to study Table 2 of Boothroyd & Sackmann (2003), who provide a list of inferred solar envelope helium abundances from a variety of calculations since 1994 using the OPAL (Rogers et al. 1996) and MHD (Däppen et al. 1988) equations of state; values as high as 0.2539 ± 0.0005 (Di Mauro et al. 2002, using the OPAL EOS), and

as low as 0.232 ± 0.006 (Kosovichev 1997, using the MHD EOS) have been derived. Guzik & Cox (1993) find a convection zone helium abundance of 0.240 ± 0.005 , using the forward method of directly comparing observed and calculated p -mode frequencies for solar models with the MHD equation of state. Shibahashi, Hiremath, and Takata (1999) find a still lower value, of ~ 0.226 (and a convection zone depth of $0.718 R_{\odot}$) using an alternate method of constructing a seismic model by solving the basic stellar structure equations imposing a helioseismically-derived sound-speed profile. These values coincidentally agree well with our enhanced-diffusion Model 5! However, Takata & Shibahashi (2003), using a more standard inversion technique, derive a seismic model with a convection-zone Y of 0.247, consistent with Basu & Antia (2004a), who use the Rogers & Nayfonov (2002) EOS. Nevertheless, given this variation of results with methods and equation of state, perhaps it is possible that a lower convection-zone helium abundance could be accommodated, as results from these enhanced-diffusion models.

5. Conclusions and Recommendations for Future Work

As discussed first by Basu & Antia (2004a), Bahcall & Pinsonneault (2004), and Turck-Chièze et al. (2004a), the new photospheric element abundances give worse agreement with helioseismology. The agreement can be improved somewhat by enhanced diffusion of elements C, N, O, Ne, & Ar relative to H and He, but not enough to restore agreement attained with the standard model, and only by large *ad hoc* changes in thermal diffusion coefficients.

We are forced to question whether something has been overlooked in the revised abundance determinations of Asplund et al. that is causing them to be systematically too low. However, their work is convincing given the consistency in the abundance determinations for a given element using several different atomic and molecular transitions, and the many improvements incorporated into the analysis.

Judging from comparisons of solar models using the OPAL and slightly lower Los Alamos National Laboratory (LANL) LEDCOP (Light-Element Detailed Configuration Opacities) opacities (Neuforge-Verheecke et al. 2001b), opacity increases of about 20% above the OPAL values for conditions just below the convection zone would nearly eliminate the discrepancies in sound speed and convection zone depth for models with the new abundances. Bahcall et al. (2004), Serenelli et al. (2004), Basu & Antia (2004a,b), and Montalbán et al. (2004) found that opacity increases of about this magnitude just below the convection zone are needed to restore the convection zone depth to the seismically-determined value. Bahcall et al. (2004) find that opacity increases of 11% between 2 and 5 million K are needed

to improve the general sound-speed profile agreement. However, the LLNL OPAL and LANL LEDCOP opacities, calculated independently with different approaches, now agree for solar conditions to within about 3% percent, correcting for differences due to interpolation (Neuforge-Verheecke et al. 2001b), with LEDCOP being lower than OPAL for the same (GN93) mixture. Badnell et al. (2005) recently evaluated the OP opacities and compared them against the OPAL opacities for the same Asplund et al. (2004) mixture, and found OP opacities only 2.5% higher than the OPAL opacities just below the convection zone, not a large enough increase to significantly improve solar model results, as reported by Antia & Basu (2005). It may be unlikely, considering this agreement between these three independent opacity calculations (LEDCOP, OPAL, and OP) that the Rosseland mean opacities for solar mixtures could be incorrect by more than several percent for conditions below the convection zone. The importance of resolving this discrepancy with helioseismology, and the large magnitude of the opacity increase required, provide motivation for opacity experiments at laser or pulsed-power facilities, as suggested by Turck-Chièze et al. (2004a).

Montalban et al. (2004) were able to restore most of the sound-speed profile agreement by adopting a combination of less severe corrections, for example 50% increases in diffusion velocities combined with $\sim 7\%$ opacity corrections, or 50% increases in diffusion velocities combined with a less-reduced convection-zone Z/X calibration (0.0195). Basu & Antia (2004a,b) were also able to restore most of the sound-speed profile agreement with less extreme abundance decreases ($Z/X = 0.0218$) and diffusion velocity multipliers (1.65). These models still had a somewhat too low convection-zone Y abundance. However, these solutions, while more physically acceptable than large changes in one quantity alone, still require changes beyond the estimated 1σ uncertainties in abundances, opacities, or diffusion rates, and are not fully satisfactory.

Antia & Basu (2005) have proposed that the Asplund et al. derived neon abundance might be too low. Neon, along with oxygen, is a significant contributor to opacity below the convection zone. Since there are no photospheric neon lines, the neon abundance is derived by determining its abundance relative to oxygen in the corona, or from energetic particles, and then scaling to the photospheric oxygen abundance. For neon alone to account for the needed opacity below the convection zone, Antia & Basu find that a factor of four increase (0.6 dex) in neon abundance is required over the Asplund et al. (2005) value, whereas the Asplund et al. (2005) quoted uncertainty is only 0.06 dex. Equivalently, smaller Ne abundance increases (by a factor of 2.5), combined with increases of C, N, and O abundance at the limits of their uncertainty (0.05 dex), also can provide the needed opacity. Whether these abundance increases are realistic remains to be investigated.

Young & Arnett (2005, in preparation), following a suggestion by Press (1981) and

Press & Rybicki (1981), are investigating whether entropy transport by waves generated near the convection-zone base provides an effective opacity that could supplement the radiative opacity. Such an opacity increase would improve sound-speed agreement below the convection zone for the standard model with the old abundances, as well as models with reduced abundances.

Considering that enhanced diffusion usually produces models with a lower convection zone Y , it would also be worthwhile to re-assess the helioseismically-inferred Y abundance taking advantage of improvements in available equations-of-state, and also using equations-of-state calculated for the new abundance mixtures. For example, perhaps the EOS of A. Irwin described in Cassisi, Salaris, & Irwin (2003) including excited states, could be applied for seismic convection-zone He abundance determinations. Lin & Däppen (2005) are working to develop an inversion technique that uses the observed element abundances and oscillation frequencies to infer the equation of state in the convection zone, which could then be applied to an improved convection-zone Y determination.

We also suggest considering the remote possibility of mass *accretion*. Perhaps a solar model could be evolved that is consistent with helioseismology if the initial $\sim 98\%$ of the Sun’s mass accumulated during its formation had higher initial element abundances, closer to the abundances of the GN93 mixture. The last $\sim 2\%$ of material accreted would need to have somewhat lower abundances of the more volatile elements, consistent with the present photospheric abundances, taking into account also a nominal rate of diffusion. The accretion would need to occur after the Sun is no longer fully convective, but it could occur very early, over a few million years after the Sun’s arrival on the main sequence; there is also no reason why this small amount of accretion could not occur over a much longer timescale, up to ~ 1 Gyr. This upper limit on timescale is estimated roughly by considering earlier studies of the amount and timescale for early solar mass loss that does not change the core H-depletion and solar structure enough to significantly worsen agreement with helioseismology (e.g., Guzik & Cox 1995; Sackmann & Boothroyd 2003). On the other hand, probably these constraints no longer apply as the helioseismic agreement is poor anyway with the new abundances! The timescale might be constrained better by determining the ages at which young G-type stars no longer show any evidence of circumstellar material to be accreted, or considering the implications for depletion of photospheric lithium in such a modified evolution scenario.

Such differentiated accretion, if it were the norm for star formation instead of an exception for the Sun, would probably have minimal impact on the rest of stellar evolution. For stars of initial mass somewhat lower than the Sun, their deeper envelope convection zones would homogenize and dilute the small amount of presumed element-depleted material accreted at late time. For stars somewhat more massive than the Sun with shallower en-

velope convection zones, the timescale for mass accretion is more rapid, which might result in less differentiation of a pre-stellar disk or nebula, the star’s more rapid rotation might homogenize any element-depleted material accreted late, and in any case diffusive settling of elements and radiative levitation already is expected to significantly decrease the surface abundances of some elements, while enhancing others. Perhaps it would be possible to find a signature of late accretion of element-depleted material by examining changing carbon-to-iron, or oxygen-to-iron abundance ratios during the first dredge-up phase for cluster stars about the mass of the Sun, as during this first dredge-up the convective envelope would deepen and homogenize the hypothesized low- Z convective region into the higher- Z material below. Because the amount of Z -depleted material to be accreted late is small compared to the stellar mass, and would be mixed with the rest of the stellar envelope during the first dredge-up, such late accretion would have minimal impact on galactic chemical evolution. The only caution, then, would be to be wary of inferring the global composition of main-sequence stars of about one solar mass from their photospheric abundances alone.

This accretion solution does not raise a problem with reconciling photospheric and meteoritic abundances of C, N, O, or Ne that we would like to decrease in the convection zone, as these elements are volatile and depleted in meteorites. However, this accretion solution would increase the difficulties of using helioseismology as a tool to probe the physics of the solar interior. We would not be able to constrain the abundances of the bulk of the Sun by photospheric observations; more parameters are introduced, including the interior mixture, accretion rate and amount. It would be extremely difficult to infer the Sun’s interior abundance by helioseismic tests alone, and decouple abundance inferences from uncertainties in opacity, diffusion treatment, or equation of state. We advocate this solution only as a last resort.

We would like to acknowledge Carlos Iglesias, John Bahcall, Nicholas Grevesse, Sylvaine Turck-Chièze, Sarbani Basu, Nicholas Grevesse, Aldo Serenelli, J. Montalban, Werner Däppen, Patrick Young, and Paul Bradley for preprints and useful discussions.

REFERENCES

- Alexander, D. & Ferguson, J. 1995, private communication
- Angulo, C. et al. 1999, Nucl. Phys. A, 656, 3
- Antia, H.M. & Basu, S. 2005, ApJ, 620, L129

- Asplund, M., Grevesse N., Sauval, A.J., Allende Prieto, C., & Kiselman, D. 2004, *A&A*, 417, 751
- Asplund, M., Grevesse N., & Sauval, A.J. 2005, in *Cosmic Abundances as Records of Stellar Evolution and Nucleosynthesis*, eds F.N. Bash and T.G. Barnes, ASP, astro-ph/0410214, v2
- Badnell, N.R., Bautista, M.A., Butler, K., Delahaye, F., Mendoza, C., Palmeri, P., Zeippen, C.J., & Seaton, M.J. 2004, astro-ph/0410744, v2
- Bahcall, J.N. & Pinsonneault M.H. 2004, *Phys. Rev. Lett.*, 92, 12
- Bahcall, J.N., Basu, S., Pinsonneault, M.H., & Serenelli, A.M. 2004, astro-ph/0407060, v2
- Bahcall, J.N., Pinsonneault, M.H., & Basu, S. 2001, *ApJ*, 555, 990
- Bahcall, J.N., Serenelli, A.M., & Pinsonneault, M.H. 2004, *ApJ*, 614, 464
- Bahcall, J.N. & Serenelli, A.M 2004, astro-ph/0412096, v1
- Basu, S. 1998, *MNRAS*, 298, 719
- Basu, S. & Antia, H.M. 1995, *MNRAS*, 276, 1402
- Basu, S. & Antia, H.M. 2004a, *ApJ*, 606, L85
- Basu, S. & Antia, H.M. 2004b, in *Helio- and Asteroseismology: Towards a Golden Future*, proc. SOHO14/GONG 2004 Workshop, ed. D. Danesy, ESA SP-559, p. 317
- Basu, S., Pinsonneault, M.H., & Bahcall, J.N. 2000, *ApJ*, 529, 1084
- Bohm-Vitense, E. 1958, *Zeitschrift fur Astrophysik*, 46, 108
- Boothroyd, A.I. & Sackmann, I.-J. 2003, *ApJ*, 583, 1004
- Brun, S., Turck-Chièze, S., & Zahn, J.-P. 1999, *ApJ*, 525, 1032
- Burgers, J.M. 1969, *Flow Equations for Composite Gases*, New York: Academic
- Cassisi, S., Salaris, M., & Irwin, A. 2003, *ApJ*, 588, 862
- Chaplin, W.J., Elsworth, Y., Isaak, G.R., Lines, R., McLeod, C.P., Miller, B.A., & New R. 1996, *MNRAS*, 282, L16
- Chaplin, W.J., Elsworth, Y., Isaak, G.R., Lines, R., McLeod, C.P., Miller, B.A., & New R. 1998, *MNRAS*, 300, 1077

- Cox, A.N. & Guzik, J.A. 2004, *ApJ*, 613, L169
- Cox, A.N., Guzik, J.A., & Kidman, R.B. 1989, *ApJ*, 342, 1187 (CGK89)
- Däppen, W., Mihalas, D., Hummer, D.G., & Mihalas, B. 1988, *ApJ*, 332, 261 (MHD)
- Di Mauro, M.P., Christensen-Dalsgaard, J., Rabello-Soares, M.C., & Basu, S. 2002, *A&A*, 384, 666
- Gabriel, M. 1997, *A&A*, 327, 771
- Garcia, R.A., et al. 2001, *Sol. Phys.*, 200, 361
- Grevesse, N. & Sauval, A.J. 1998, *Spa. Sci. Rev.*, 85, 161 (GS98)
- Grevesse, N. & Noels, A. 1993, in *Origin and Evolution of the Elements*, ed. N. Prantzos, E. Vangioni-Flam, & M. Cassè, Cambridge U. Press, 15 (GN93)
- Guzik, J.A. & Watson, L.S. 2004, in *Helio- and Asteroseismology: Towards a Golden Future*, proc. SOHO14/GONG 2004 Workshop, ed. D. Danesy, ESA SP-559, 456
- Guzik, J.A. & Swenson, F.J. 1997, *ApJ*, 491, 967
- Guzik, J.A. & Cox, A.N. 1993, *ApJ*, 411, 394
- Guzik, J.A. & Cox, A.N. 1995, *ApJ*, 448, 905
- Iglesias, C. & Rogers, F.J. 1996, *ApJ*, 484, 943
- Guenther, D.B., Demarque, P., Kim, Y.C., & Pinsonneault, M.H. 1992, *ApJ*, 387, 372
- Kosovichev, A.G. 1997, in *AIP Conf. Proc. 385, Robotic Exploration close to the Sun: Scientific Basis*, ed. S.R. Habbal (Woodbury: AIP), 159
- Lin, C.-H. & Däppen, W. 2005, *ApJ*, 623, in press
- Lodders, K. 2003, *ApJ*, 591, 120
- Montalban, J., Miglio, A., Noels, A., Grevesse, N., & Di Mauro, M.P. 2004, in *Helio- and Asteroseismology: Towards a Golden Future*, proc. SOHO14/GONG 2004 Workshop, ed. D. Danesy, ESA SP-559, 574, astro-ph/0408055, v2
- Morel, P., Provost, J., & Berthomieu, G. 1997, *A&A*, 327, 349
- Neuforge-Verheecke, C., Goriely, S., Guzik, J.A., Swenson, F.J., & Bradley, P.A. 2001a, *ApJ*, 550, 493

- Neuforge-Verheecke, C., Guzik, J.A., Keady, J.J., Magee, N.H., Bradley, P.A., & Noels, A. 2001b, *ApJ*, 561, 450
- Pesnell, W.D. 1990, *ApJ*, 363, 227
- Press, W.H. 1981, *ApJ*, 245, 286
- Press, W.H. & Rybicki, G.B. 1981, *ApJ*, 248, 751
- Rogers, F.J., Swenson, F.J., & Iglesias, C.A. 1996, *ApJ*, 456, 902
- Rogers, F.J., and Nayfonov, A. 2002, *ApJ*, 576, 1064.
- Richard, O., Vauclair, S., Charbonnel, C., & Dziembowski, W. 1996, *A&A*, 312, 1000
- Sackmann, I.-J. & Boothroyd, A.I. 2003, *ApJ*, 583, 1024
- Schou, J., & Tomczyk, S. 1996, m2 table, <http://www.hao.ucar.edu/public/research/mlso/LowL/data.html>
- Serenelli, A.M., Bahcall, J.N., Basu, S., & Pinsonneault, M.H. 2004, in *Helio- and Asteroseismology: Towards a Golden Future*, proc. SOHO14/GONG 2004 Workshop, ed. D. Danesy, ESA SP-559, 623
- Seaton, M.J. & Badnell, N.R. 2004, *MNRAS*, 354,457
- Shibahashi, H., Hiremath, K.M., & Takata, M. 1999, *Adv. Space Res.*, 24 177
- Takata, M. & Shibahashi, H. 2003, *Publ. Astron. Soc. Japan* 55, 1015
- Théado, S., Vauclair, S., & Richard, O. 2001, proc. SOHO10/GONG 2000 Workshop, ESA SP-464, 547
- Toutain, T., Appourchaux, T., Frölich, C., Kosovichev, A.G., Nigam, R., & Scherrer, P.H. 1998, *ApJ*, L147
- Turcotte, S., Richer, J., Michaud, G., Iglesias, C.A., & Rogers, F.J. 1998, *ApJ*, 504, 539
- Turck-Chièze, S., Couvidat, S., Piau, L., Ferguson, J., Lambert, P., Ballot, J., Garcia, R.A., & Nghiem, P. 2004a, *Phys. Rev. Lett.* 93, 211102
- Turck-Chièze, S., Garcia, R.A., Couvidat, S., Ulrich, R.K., Bertello, L., Varadi, F., Kosovichev, A.G., Gabriel, A.H., Berthomieu, G., Brun, A.S., Lopes, I., Pallé, P., Provost, J., Robillot, J.M., & Roca Cortés, T. 2004b, *ApJ*, 604, 455

Turck-Chièze, S., Garcia, R.A., Couvidat, S., Ulrich, R.K., Bertello, L., Varadi, F., Kosovichev, A.G., Gabriel, A.H., Berthomieu, G., Brun, A.S., Lopes, I., Pallé, P., Provost, J., Robillot, J.M., & Roca Cortés, T. 2004c, *ApJ*, 608, 610

Turck-Chièze, S., Garcia, R.A., Couvidat, S., et al. 2004d, in *Helio- and Asteroseismology: Towards a Golden Future*, proc. SOHO14/GONG 2004 Workshop, ed. D. Danesy, ESA SP-559, 85

Young, P.A. & Arnett, D. 2005, in preparation

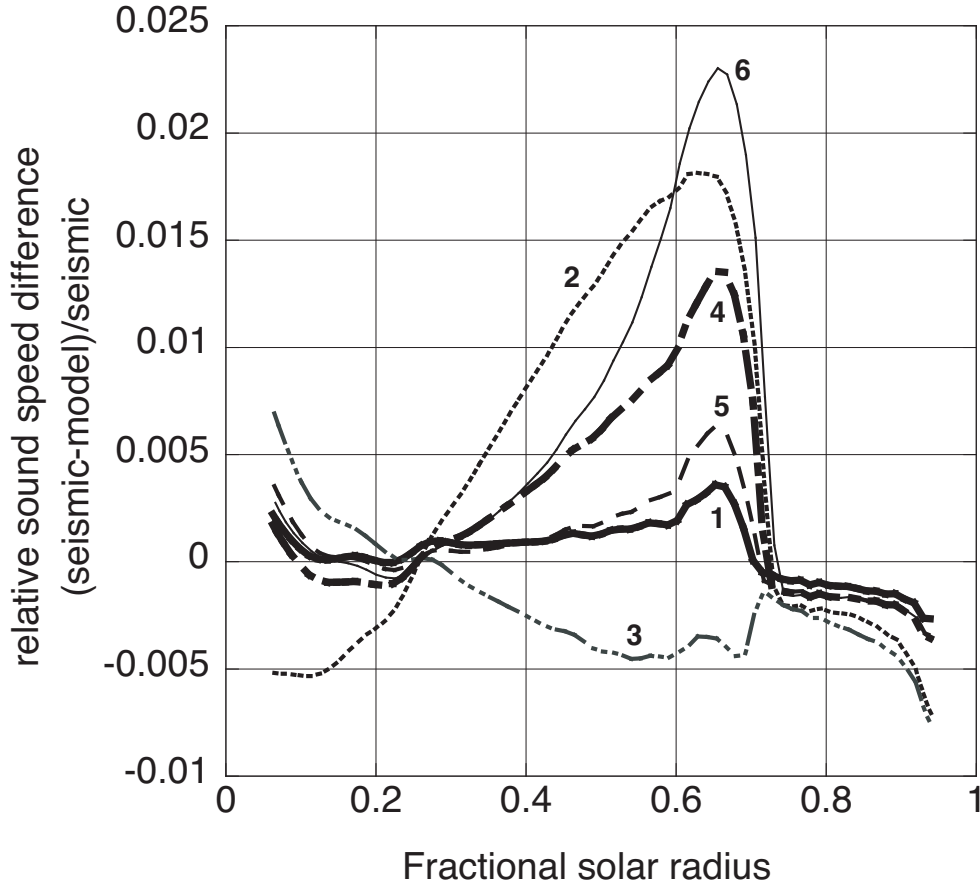


Fig. 1.— Sound-speed profile differences $[(\text{seismic-model})/\text{seismic}]$ for six models. Seismic inversion from Basu et al. (2000). Thick solid: Standard Model 1; dot: No Diffusion Model 2; dash triple-dot: Enhanced Diffusion Model 3; thick dash-dot: Enhanced Z-Diffusion Model 4; dash: Intermediate Enhanced Diffusion Model 5; thin solid: High-Z Enhanced Diffusion Model 6.

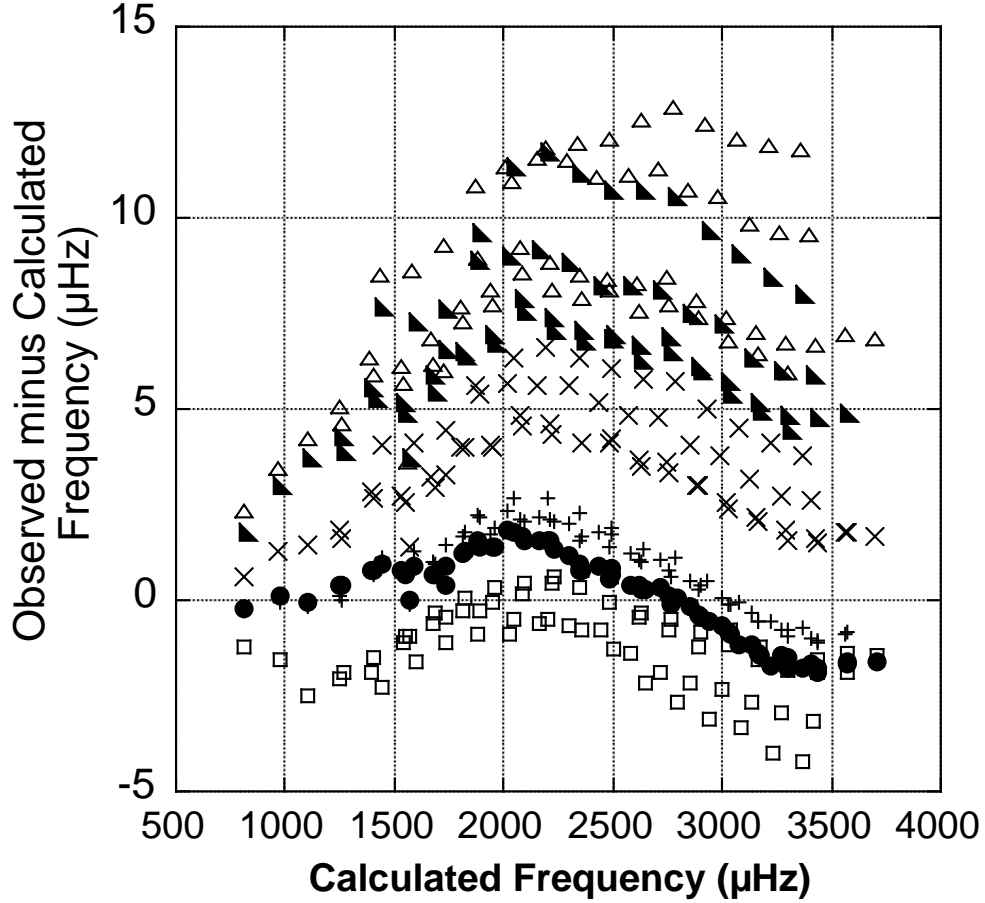


Fig. 2.— Observed minus calculated versus calculated frequencies for p -modes of degree $\ell=0, 2, 10,$ and 20 . Observations are from either BiSON (Chaplin et al. 1996, 1998) or LowL (Schou & Tomczyk 1996), supplemented by a few low-frequency low-degree $\ell=0$ and $\ell=2$ modes from GOLF (Garcia et al. 2001) or SOHO/MDI (Toutain et al. 1998) data. Filled circles: Standard Model 1; open triangles: No-Diffusion Model 2; squares: Enhanced Diffusion Model 3; crosses: Enhanced Z-Diffusion Model 4; pluses: Intermediate Enhanced Diffusion Model 5; filled triangles: High-Z Enhanced Diffusion Model 6.

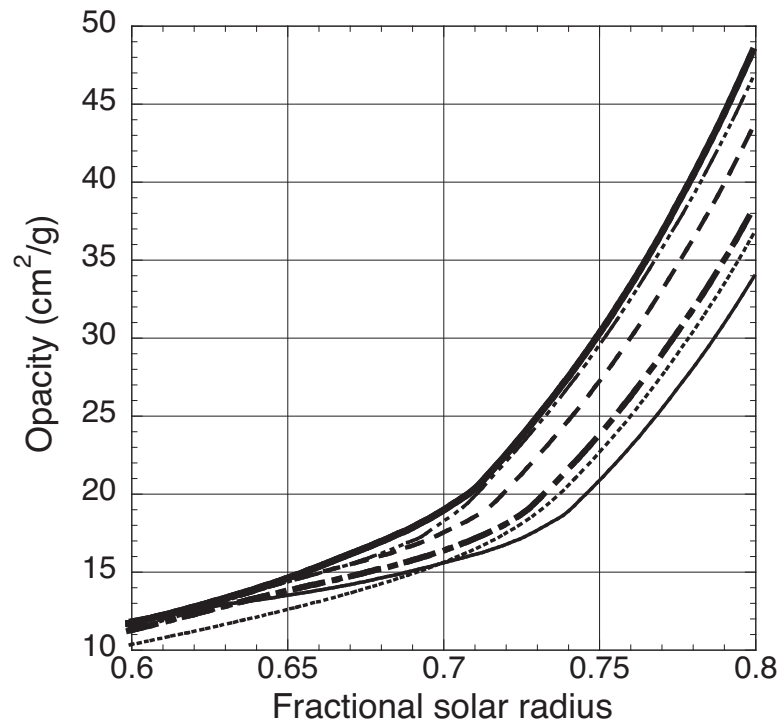


Fig. 3.— Opacity versus fractional solar radius near convection-zone base for six models. Thick solid: Standard Model 1; dot: No Diffusion Model 2; dash triple-dot: Enhanced Diffusion Model 3; thick dash-dot: Enhanced Z-Diffusion Model 4; dash: Intermediate Enhanced Diffusion Model 5; thin solid: High-Z Enhanced Diffusion Model 6.

Table 1. Properties of Evolved Solar Models

Property	Model 1 Standard GN93	Model 2 Low-Z No Diffusion	Model 3 Enhanced Diffusion	Model 4 Enhanced Z-Diffusion	Model 5 Intermediate Enhanced Diffusion	Model 6 High-Z Enhanced Diffusion
$Y_{\text{init.}}$	0.2703	0.2493	0.2626	0.2650	0.2705	0.2870
$Z_{\text{init.}}$	0.0197	0.01425	0.0197	0.0197	0.0197	0.0240
$Y_{\text{conv. zone}}$	0.2419	0.2493	0.1926	0.2339	0.2269	0.2541
$Z_{\text{conv. zone}}$	0.01805	0.01425	0.01552	0.01400	0.01561	0.01268
Z/X	0.0244	0.0194	0.0196	0.0186	0.0206	0.0173
α^{a}	1.769	1.560	1.944	1.658	1.763	1.547
$R_{\text{conv. zonebase}} (R_{\odot})$	0.7133	0.7388	0.7022	0.7283	0.7175	0.7406
$T_{\text{central}} 10^6 \text{ K}$	15.66	15.21	15.83	15.69	15.79	16.13
Cl ν flux SNU	7.78	4.80	9.12	7.90	8.72	11.83
Ga ν flux SNU	128.1	112.1	129.1	135.0	132.8	149.9
Super K ν flux SNU	1.02	0.597	1.03	1.16	1.16	1.58

^a α is the mixing-length to pressure-scale-height ratio

Table 2. Enhanced Diffusion Models Compared

Property	Basu & Antia FULL1M	Basu & Antia FULL2M	Montalban et al. D1	Montalban et al. D4	Guzik et al. Model 3	Guzik et al. Model 4	Guzik et al. Model 5
Diffusion Multiplier	1.65	1.65	1.5	2	3 ^a	7 ^a ; 1 ^b	4 ^a ; 1.5 ^b
Z/X	0.0171	0.0218	0.0195	0.0177	0.0196	0.0186	0.0206
$Y_{\text{conv. zone}}$	0.2244	0.2317	0.241	0.226	0.1926	0.2339	0.2269
$R_{\text{conv. zonebase}}(R_{\odot})$	0.7233	0.7138	0.717	0.714	0.7022	0.7283	0.7175

^ainverse of multiplier on element thermal resistance coefficient relative to H, He

^binverse of multiplier on helium thermal resistance coefficient relative to H and other elements

Table 3. Predicted g-mode and radial mode frequencies (μHz) and growth rates^a

Mode	Obs.	Model 1	Model 2	Model 3	Model 4	Model 5	Model 6
$\ell=1, \text{g}_1$	262.1 ^b	260.6 (3.3)	251.8 (2.2)	266.6 (5.3)	259.6 (3.1)	262.2 (8.5)	256.8 (2.8)
$\ell=2, \text{g}_3$	220.7 ^c	221.5 (1.5)	248.9 (3.3)	225.7 (1.6)	220.8 (1.6)	222.5 (1.6)	219.5 (1.8)
F		257.9 (13)	261.8 (17)	256.1 (12)	259.6 (15)	258.2 (14)	260.8 (16)
1H		403.9 (32)	403.8 (37)	403.7 (30)	403.2 (34)	403.5 (32)	401.8 (35)
2H		535.4 (124)	534.3 (142)	535.6 (116)	535.0 (130)	535.3 (124)	534.4 (135)
3H		680.2 (444)	677.6 (493)	681.0 (411)	678.9 (453)	680.0 (437)	677.4 (463)
4H		825.1 (1499)	822.5 (1581)	826.3 (1289)	824.3 (1446)	825.2 (1390)	823.0 (1489)
5H	972.6 ^d	972.5 (4096)	969.2 (4421)	974.2 (3720)	971.4 (4053)	972.7 (3958)	970.0 (4107)

^aGrowth rates in parentheses, 10^{-10} per period; time-dependent convection not included

^bTurck-Chièze et al. (2004b,c); observed singlet, possible $\ell=1$

^cTurck-Chièze et al. (2004b,c); observed triplet, 220.12, 220.72, and 221.26 μHz ; probable $\ell=2$

^dTurck-Chièze et al. (2004d)